Thermochimica Acta 513 (2011) 43–48

Contents lists available at ScienceDirect

Thermochimica Acta

journal homepage: www.elsevier.com/locate/tca

# Thermochemistry and kinetics of silica dissolution in NaOH aqueous solution

Meriem Fertani-Gmati, Mohamed Jemal*

*Tunis-El Manar University, Faculty of Science, Chemistry Department, Applied Thermodynamics Laboratory, 2092 Tunis El Manar, Tunisia*

ARTICLE INFO

*Article history:*
Received 29 June 2010
Received in revised form 29 October 2010
Accepted 2 November 2010
Available online 12 November 2010

*Keywords:*
Silica dissolution
Microcalorimetry
Thermochemistry
Kinetics
Isoconversional model

ABSTRACT

Dissolution of increasing amounts of silica (α-cristobalite) in the same volume of a 4% weight of sodium hydroxide solution was followed by microcalorimetry in a closed cell at temperature up to 130 °C. The process led to the formation of a dissolved entity whose formula depends on the $Na_2O/SiO_2$ ratio. At the beginning dissolution gave [$3Na_2O$, $4SiO_2$] entity and when increasing dissolved silica amounts, the latter transforms into [$Na_2O$, $2SiO_2$]. Kinetic study showed that dissolution starts by a very rapid step with about 10% of the whole heat energy released and continued with a very slow process. Kinetic analysis showed that the latter agrees with two successive silica first-order reactions scheme. The resulting activation energy values are of the same magnitude order of that deduced from the isoconversional model.



## 1. Introduction

In the wet manufacture process of phosphoric acid, the attack of phosphate ore by the mixture of phosphoric and sulfuric acids leads to concentrated phosphoric acid containing various amounts of impurities which were present in the ore or in the reagents used in the process.

Usually, the impurities elimination is done by neutralizing the acid with sodium hydroxide. Iron, aluminum and magnesium are eliminated at 97%, 75% and 63%, respectively, but losses of $P_2O_5$ are important and can reach up to 10%. An alternative way to reduce $Mg^{2+}$, $Fe^{3+}$ and $Al^{3+}$ contents consists in precipitating them as insoluble silicate salts. The first step of this process is to prepare solutions of alkali silicates to be added to manufactured phosphoric acid. This paper aimed to follow the dissolution of a variety of silica (α-cristobalite) in NaOH aqueous solution at different temperatures in order to get information on its solubility. But as it will be seen later, silica dissolution is a very complex process.

Several authors have been interested in silica dissolution and proposed different models since the 1950s [1,2]. The work of Bulteel et al. [3] which was performed on the alkali–silica reaction showed that the process began with a break of the siloxane bond (Si–O–Si). According to this team, the predominant species in alkaline solution is $SiO_{5/2}^-$. Attack of the latter by a hydroxyl ion gives the anion $H_2SiO_4^{2-}$ which is in equilibrium with $H_3SiO_4^-$ (Iler equilibrium [4]). Dove and Crerar [5] suggested that the silica surface, represented as ≡Si–O–Si≡, reacts in contact with water to form two (≡Si–OH) species which move into ≡Si–$O^-$ in basic solutions. Dron and Brivot [6] consider the equilibrium between the hydrated silica surface and the silicic acid in solution. The surface interaction has been described by the following reaction:

$$SiO_2, H_2O_{surf} + H_2O \rightarrow (H_4SiO_4)_{solution}$$

Dissolution of silica involves several silicate species, including the existence of oligomers. According to many authors [7–9], the process starts by combining two molecules of $Si(OH)_4$ to form $Si_2O_7H_6$ with a siloxane bond (Si–O–Si) and the formation of dimers can increase as pressure and temperature increase. The dimer can be linked to other $Si(OH)_4$ to form higher order oligomers and those having more than 3 atoms of Si can move into cyclic structures or into more complex forms leading to an infinite variety of polymers [10]. The presence of several polymeric species has been reported since the 1950s [11,12]. Using a [$^{29}$Si] NMR analysis, Harris et al. [13] distinguished 11 types of oligomers in a concentrated solution of potassium silicate. The dominant species depend strongly on experimental conditions [14]. The main species present in aqueous solution at low pH seem to be monomeric ($H_4SiO_4$(aq), $H_3SiO_4^-$ and $H_2SiO_4^{2-}$) [15,16]. For pH greater than 10, a wide variety of polymers formed in solution, up to hexameric species [17].

Felmy et al. [18] studied the silicate polymers and distinguished 8 different species. They showed that in a solution containing sodium ions the formation constants of species with the same number of silicon are very close and the linear and cyclic species have similar structures (especially trimers and tetramers). Moreover, sodium in solution changes the linear chains, forming a sort of bridge between the end chain oxygens. These authors also con-

* Corresponding author. Tel.: +216 98 90 27 71; fax: +216 71 88 34 24.
*E-mail address:* jemal@planet.tn (M. Jemal).

0040-6031/$ – see front matter © 2010 Elsevier B.V. All rights reserved.
doi:10.1016/j.tca.2010.11.008

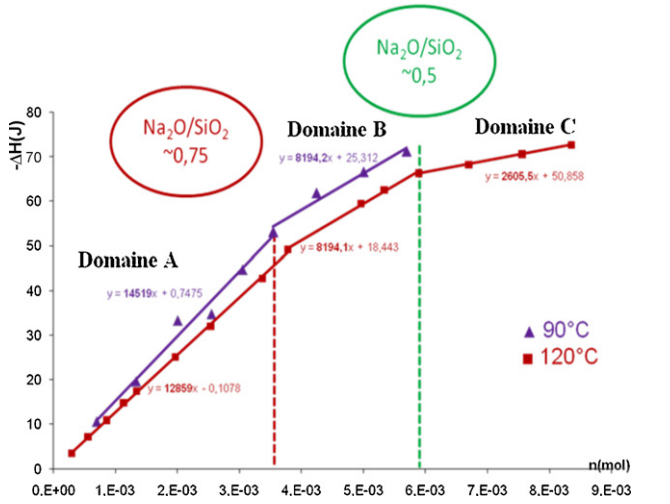


**Fig. 1.** Heat energy measured by integrating the raw signal as a function of the added silica moles number in 5 mL of 4% weight NaOH aqueous solution at 90 and 120 °C.

cluded that various forms of trimers and tetramers had roughly the same thermodynamic stability. According to Trinh et al. [19], the condensation reaction occurs either through anion or neutral species. The "anionic" mechanism seems to be more favorable kinetically and to occur in two steps which are the formation of Si–O–Si between two molecules followed by the elimination of a water molecule.

## 2. Experimental

Commercial silica (Fluka) was dissolved in an aqueous solution having 4% weight NaOH. The dissolution experiments are conducted in a C-80 Setaram Calorimeter, at isothermal conditions using the reversal cells in shaking mode. Various amounts of silica were placed in the lower compartment of the cell and a constant volume of NaOH (5 mL) in the upper compartment which was separated from the former by a metallic cover. After one night of stabilization time, the reactants were mixed by the reversal system and the dissolution was followed until equilibrium which was sometimes obtained after a very long time (up to 4 days) under shaking. The solid mass is fixed between 17 and 500 mg and the temperature at 80–130 °C.

## 3. Thermodynamics

In case of a simple process, the heat evolved by dissolving increasing amounts of solid in the same volume of solvent increases or decreases continuously until saturation from which it becomes constant. It is not so simple with silica and the phenomenon is exothermic whatever the mass of dissolved solid and the temperature (curve a in Fig. 2). Fig. 1 shows the drawing of the heat energy released at 90 and 120 °C by dissolving successively 17–500 mg of silica in 5 mL of NaOH solution. One can notice 3 line segments at 120 °C and 2 at 90 °C noted as A, B and C domains respectively. Experiments were not performed in C domain at 90 °C because of the very long duration of the process. The higher the amount of solid and lower the temperature, the longer the duration.

Table 1 gathers the molar dissolution enthalpy in various domains with the corresponding errors calculated considering the scatter around the least square line. One can notice the same value of $\Delta H$ in B domain and slight variation in A domain.

X-ray diffraction analysis of the solid isolated at high temperature (120 °C) and different reaction times (3 min, 1 h, 2 h, 4 h and 22 h) showed only the presence of undissolved silica.

**Table 1**
Molar enthalpy of dissolution of silica in NaOH solution at 90 and 120 °C.

| | $\Delta H$ (J mol$^{-1}$) at 90 °C | $\Delta H$ (J mol$^{-1}$) at 120 °C |
|---|---|---|
| Domain A | 14,519 ± 920 | 12,859 ± 145 |
| Domain B | 8194 ± 620 | 8194 ± 51 |
| Domain C | – | 2605 ± 17 |

Along one domain, the molar enthalpy is constant and so each domain corresponds to the same process. Fig. 1 shows that A domain lies still $Na_2O/SiO_2$ ratio near 0.75 and so it corresponds to the formation of dissolved entity $[3Na_2O, 4SiO_2]$. Molar $Na_2O/SiO_2$ ratio for B domain lies between 0.75 and 0.5. This corresponds to the transformation of the previous entity to $[Na_2O, 2SiO_2]$ in the dissolved state, according to the reaction:

$$[3Na_2O, 4SiO_2]_{diss} + 2SiO_2 \rightarrow 3[Na_2O, 2SiO_2]_{diss}.$$

## 4. Kinetics

In preliminary experiments, the time constants of the reaction cell were determined using a pair of cells which were previously provided with two electrical resistances in order to perform calibration operation in the same conditions as for the chemical process [20]. Values of these constants were then used to calculate the deconvoluted curve (or thermogenesis curve) from the raw signal resulting from chemical process. The two signals differ or superpose depending on the speed of the corresponding phenomenon. This procedure allowed to propose kinetic schemes for the attack of synthetic phosphates [20,21] or a phosphate ore [22] by acid solutions. Fig. 2 gives an example showing a large difference at the beginning between the signals which superpose when time elapses and the process becomes slow.

The deconvoluted signal contains 2 peaks corresponding to exothermic phenomena whatever the temperature and the mass of dissolved solid. Nevertheless, one can notice a large difference between the peak intensities, indicating a very rapid first phenomenon with a heat energy not exceeding 10% of the whole heat energy. The kinetic study has been undertaken only for the A domain because of the complexity of the process in the other domains.

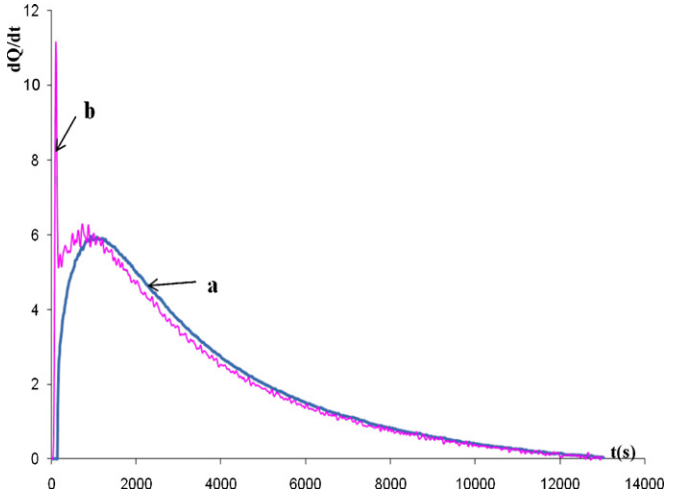


**Fig. 2.** Raw (a) and deconvoluted (b) signals corresponding to dissolution of 152 mg of silica at 120 °C.

**Table 2**
*k* and *n* parameters corresponding to domains I and II at 90 and 120 °C.

| $T$ (°C) | | 90 °C | | | | 120 °C | | | |
|---|---|---|---|---|---|---|---|---|---|
| $m_{silice}$ (mg) | | 80.345 | 120.605 | 183.375 | 212.910 | 80.725 | 152.310 | 202.575 | 227.02 |
| Domain I | $k$ | $4.61^{E-4}$ | $4.68^{E-4}$ | $2.69^{E-4}$ | $3.57^{E-4}$ | $7.24^{E-3}$ | $3.31^{E-3}$ | $2.12^{E-3}$ | $2.19^{E-3}$ |
| | $n$ | 3.68 | 4.39 | 3.18 | 4.95 | 4.36 | 3.05 | 4.13 | 4.52 |
| Domain II | $k$ | $2.73^{E-5}$ | $2.73^{E-5}$ | $2.09^{E-5}$ | $1.94^{E-5}$ | $3.18^{E-4}$ | $2.95^{E-4}$ | $2.02^{E-4}$ | $2.25^{E-4}$ |
| | $n$ | 1.26 | 1.23 | 1.22 | 1.28 | 0.84 | 1.09 | 1.16 | 1.21 |

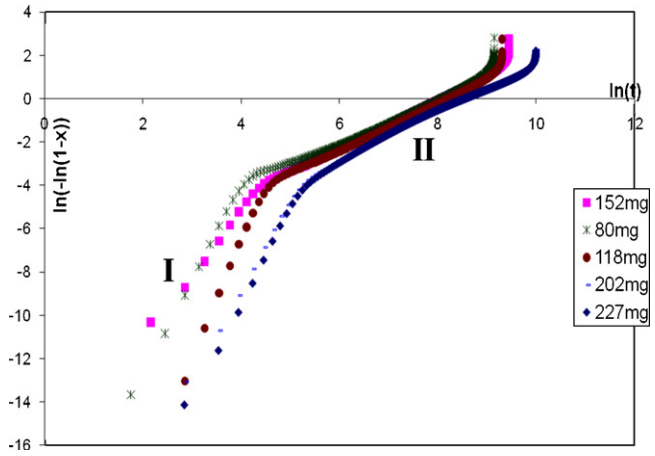


**Fig. 3.** Plot of $\ln(-\ln(1-x))$ versus $\ln(t)$ for various masses of silica dissolved in NaOH solution at 120 °C.

### 4.1. Avrami model

At the origin Avrami model has been formulated for crystallization from pure liquid [23]. It has been then extended to chemical processes [24–26]. This model links the reactant transformed fraction $x$ to time $t$ by the following equation:

$$-\ln(1-x) = kt^n \tag{1}$$

with $k$ and $n$ the Avrami constants and $x$ equals the ratio of the heat $q$ released at time $t$ over the overall heat $Q_t$ determined by integrating the whole peak. This ratio was calculated by dividing the corresponding surface areas under the peak.

Avrami parameters and successive steps in the global process can be deduced from the drawing of $\ln(-\ln(1-x))$ versus $\ln(t)$.

Fig. 3 shows 2 line segments corresponding to I and II domains respectively. According to literature [27–29], the change of the slope can be attributed to the appearance of a new phenomenon or a change of mechanism in a phase transition and so each domain corresponds to a predominant phenomenon.

Table 2 gathers the values of $k$ and $n$ parameters calculated in domains I and II for different masses of silica dissolved at 90 and 120 °C.

Parameter $n$ lies in the range {3.18–4.39} at 90 °C and {3.05–4.52} at 120 °C for the I domain and in the range {1.22–1.28} at 90 °C and {0.84–1.16} at 120 °C for II domain. So, the predominant phenomenon appearing at 90 °C in a certain domain seems to be the same at 120 °C for the same domain.

This model permits also to detect the starting time of the second phenomenon (Table 3). This time could not be detected directly from the crude or deconvoluted curves because of the overlapping of the peaks. However, this time is very short compared to the entire duration of the experiment which can last up to 4 days as it was said previously and increases as the dissolved silica amount increases and temperature becomes lower. At constant temperature, the first phenomenon seems to end earlier for small amounts of dissolved solid, its rate is highly dependent on temperature, consequently it may correspond to a bulk phenomenon.

### 4.2. Isoconversional model

In heterogeneous kinetics, the process occurring at the interface is not usually a one step reaction because of the modification of the solid surface over time leading to changes in mechanism [30–32]. This complex behavior is shown through isoconversional model. According to that model, the converted fraction $\alpha$ of a reactant is expressed as a function of time by the equation:

$$\frac{d\alpha}{dt} = kf(\alpha) \tag{2}$$

with $k$ the rate constant and $f(\alpha)$ a function associated to the mechanism.

Integration of Eq. (1) leads to:

$$g(\alpha) = \int_0^{\alpha} \frac{d\alpha}{f(\alpha)} \tag{3}$$

or

$$g(\alpha) = kt \tag{4}$$

Using the Arrhenius law, $g(\alpha)$ can be expressed as:

$$g(\alpha) = A \exp\left(-\frac{E_a}{RT}\right) t \tag{5}$$

and so:

$$\ln(t) = \frac{E_a}{RT} + \ln\left(\frac{g(\alpha)}{A}\right) \tag{6}$$

At a certain mole fraction, $\ln(g(\alpha)/A)$ is constant [33] and so it is possible to determine the activation energy, whatever the model [33], by plotting $\ln(t)$ versus $1/T$. Examples of plots of $\ln(t)$ versus $1/T$ ($80 \le T \le 130$ °C) are illustrated in Fig. 4 for different conversion rates ($0.06 \le \alpha \le 0.93$).

For a one step process, the activation energy is constant along all the process, but in the present case, the whole activation energy varies considerably as the reaction progresses suggesting the occurrence in several steps [34]. Fig. 5 shows the variation of the activation energy as a function of $\alpha$ with the errors calculated by considering the scatter of the points around the least square line drawn for each value of $\alpha$ in Fig. 4.

**Table 3**
The starting time of the second peak at 90 and 120 °C.

| $T$ (°C) | 90 °C | | | | 120 °C | | | |
|---|---|---|---|---|---|---|---|---|
| $m_{silice}$ (mg) | 80.345 | 120.605 | 183.375 | 254.675 | 80.725 | 152.310 | 202.575 | 227.020 |
| Starting time of the 2nd peak (s) | 493 | 645 | 773 | 830 | 58 | 82 | 180 | 192 |

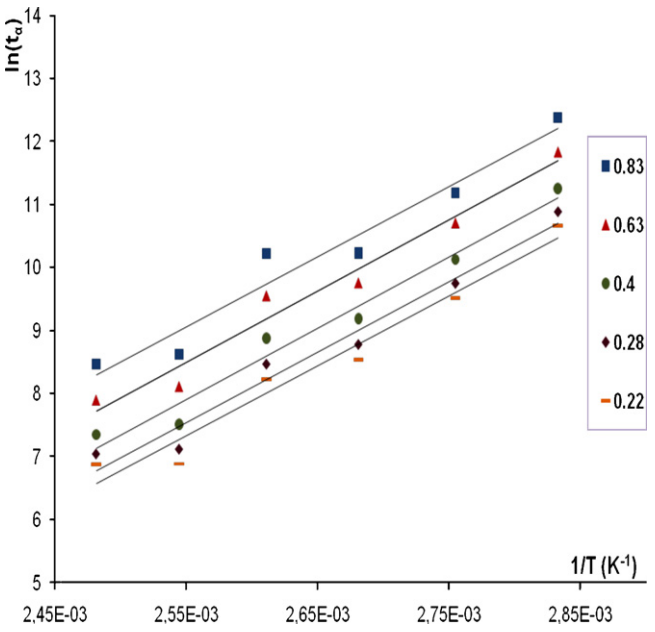


**Fig. 4.** Examples of plots of $\ln(t)$ versus $1/T$ for $80 \leq T \leq 130\,^{\circ}C$ at different $\alpha$.

The increase of the activation energy over the conversion rate has been attributed to a kinetic scheme involving consecutive [35] or parallel [36] reaction processes with limit values of activation energy. Fig. 5 shows that the whole activation energy starts at about 86 kJ mol$^{-1}$, reaches a maximum at 95 kJ mol$^{-1}$ for $\alpha = 0.55$ then decreases to about 88 kJ mol$^{-1}$.

### 4.3. Kinetic scheme

Due to the predominance of the second peak, the kinetic scheme has only considered for the latter. Different reaction schemes have been supposed for this peak in A domain and the corresponding heat flow equations have been derived then processed iteratively in order to get the overlapping of the calculated and the deconvoluted curves. Calculation indicated that the mechanism involving two successive silica first-order reactions leads to better results.

According to this model, silica (A) reacts with a sodium hydroxide solution (sol) to form a B entity which transforms into C, according to the following reaction scheme:

$$A + sol \xrightarrow{k_1} B \quad (I)$$

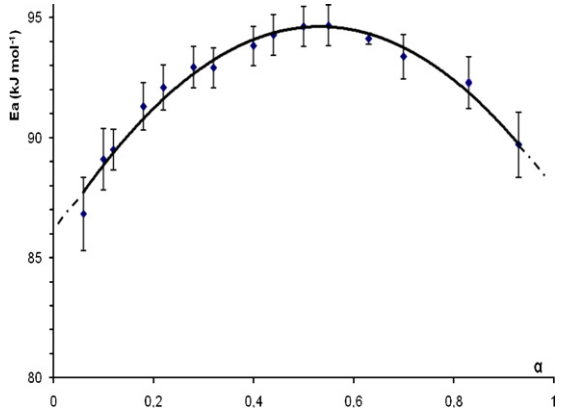


**Fig. 5.** Dependence of the activation energy versus the conversion degree calculated according to the isoconversional model.

with $k_1$ the rate constant and $\Delta H_1$ molar reaction enthalpy.

$$B \xrightarrow{k_2} C \quad (II)$$

with $k_2$ the rate constant and $\Delta H_2$ molar reaction enthalpy.

The rate equations are expressed as:

$$r_1 = k_1[A] \quad (7)$$

and

$$r_2 = k_2[B] \quad (8)$$

with $[A]$ the concentration of silica at "$t$" time if it were dissolved and $[B]$ that of $B$.

If one supposes the rate of the first reaction not be influenced by the second reaction, the concentration of $A$ is given by the following equation:

$$[A] = [A]_0 \exp(-k_1 t) \quad (9)$$

with $[A]_0$ the initial concentration of $A$.

The rate of presence of $B$ in the reactional medium is expressed as:

$$r(B) = r_1 - r_2 \quad (10)$$

and so

$$-\frac{d[B]}{dt} = k_2[B] - k_1[A] \quad (11)$$

Integrating Eq. (11) leads to:

$$[B] = [A]_0 \frac{k_1}{k_1 - k_2}[\exp(-k_2 t) - \exp(-k_1 t)] \quad (12)$$

Taking into account the mass conservation of silica, the sum of the concentrations of A, B and C species equals to the initial concentration of reactant $A$:

$$[A] + [B] + [C] = [A]_0$$

Thus

$$[C] = [A]_0 \left[1 - \frac{k_2 \exp(-k_1 t) - k_1 \exp(-k_2 t)}{k_2 - k_1}\right] \quad (13)$$

The heat $q_1$ released during the transformation of $A$ into $B$ is written as:

$$q_1 = ([A]_0 - [A])V\Delta H_1 \quad (14)$$

with $V$ the medium volume and $\Delta H_1$ the molar enthalpy of the reaction (I).

The heat of transformation of $B$ into $C$, $q_2$, is expressed as:

$$q_2 = [C]\, V\Delta H_2 \quad (15)$$

with $\Delta H_2$ the molar enthalpy of reaction (II).

The overall heat $q$ is:

$$q = q_1 + q_2$$

The heat flow can then be derived as follows:

$$\frac{dq}{dt} = \frac{m_A}{M_A}\left[\frac{\Delta_2 H\, k_1\, k_2}{k_1 - k_2}(\exp(-k_2 t) - \exp(-k_1 t)) + \Delta_1 H\, k_1 \exp(-k_1 t)\right] \quad (16)$$

Iteration has been conducted on Eq. (16) for similar masses of dissolved silica (~150 mg) at different temperatures (80–130 °C). Fig. 6 shows an example of coincidence between the theoretical and deconvoluted curves and kinetic and the resulting thermochemical parameters are compiled in Table 4.

The rate constants increase as the temperature increases and the sum of enthalpies ($\Delta H_1 + \Delta H_2$) deduced from iteration differs

**Table 4**
Kinetic and thermochemical parameters deducted from the iteration of Eq. (16) for similar masses of dissolved silica (~150 mg) at different temperatures (80–130 °C).

| Temperature (°C) | 80 | 90 | 100 | 110 | 120 | 130 |
|---|---|---|---|---|---|---|
| Mass (mg) | 152.105 | 153.110 | 154.765 | 150.585 | 152.301 | 155.095 |
| $k_1$ ($s^{-1}$) | $4.83^{E-5}$ | $7.77^{E-5}$ | $4.01^{E-4}$ | $1.13^{E-3}$ | $1.76^{E-3}$ | $5.24^{E-3}$ |
| $k_2$ ($s^{-1}$) | $9.85^{E-6}$ | $1.91^{E-5}$ | $3.73^{E-5}$ | $9.03^{E-5}$ | $2.58^{E-4}$ | $5.11^{E-4}$ |
| $\Delta H_1$ (kJ $mol^{-1}$) | 1.39 | 3.76 | 1.17 | 0.49 | 1.51 | 0.56 |
| $\Delta H_2$ (kJ $mol^{-1}$) | 18.78 | 13.95 | 13.61 | 13.71 | 10.03 | 10.56 |
| $\Delta H_1 + \Delta H_2$ (kJ $mol^{-1}$) | 20.17 | 17.71 | 14.78 | 14.20 | 11.54 | 11.12 |
| $\Delta H_{Tmes}$ (kJ $mol^{-1}$) | 22.07 | 19.61 | 13.38 | 14.36 | 11.24 | 9.55 |

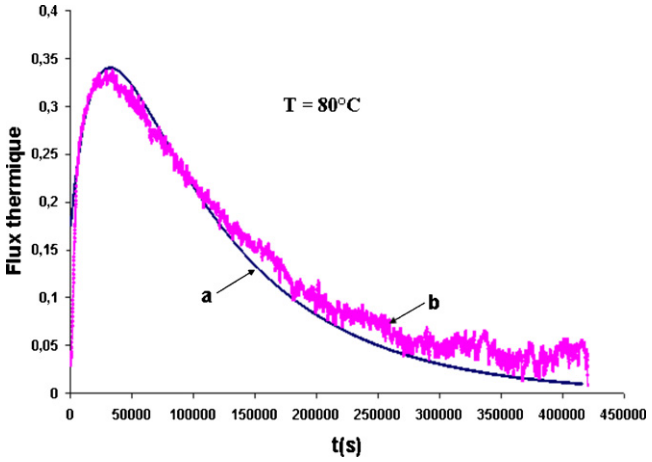


**Fig. 6.** Iteration results of Eq. (16) (curve a) and thermogenesis (curve b) of the second peak for 152 mg of silica at 80 °C.

by no more than 10% from the experimental value calculated by integrating the rough peak, except at 130 °C (15%).

Activation energies of the reaction steps were determined from the Arrhenius plot corresponding to each reaction (Fig. 7).

From the slopes of the lines, the molar activation energies have been deduced as $114.5 \pm 0.9$ kJ $mol^{-1}$ and $98.0 \pm 0.7$ kJ $mol^{-1}$ for the first and the second reaction respectively. These values confirm that the process is controlled by chemical reactions and differ from their corresponding values determined by isoconversional model by about 13 and 16.5% respectively.

Iteration has been conducted for different masses of dissolved silica at 90 and 120 °C. Table 5 gathers the results obtained at 120 °C.

One can notice that the rate constants remain very similar for different masses of silica and the measured ($\Delta H_{Tmes}$) and calculated

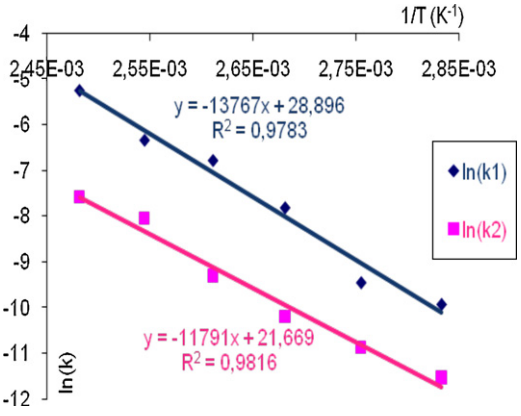


**Fig. 7.** The plot of $\ln(k_1)$ and $\ln(k_2)$ versus $(1/T)$.

**Table 5**
Kinetic and thermochemical parameters deducted from the iteration of Eq. (16) in A domain for different masses of dissolved silica at 120 °C.

| Mass (mg) | 80.725 | 118.165 | 152.310 | 202.600 | 227.020 |
|---|---|---|---|---|---|
| $k_1$ ($s^{-1}$) | $1.41^{E-3}$ | $1.36^{E-3}$ | $1.76^{E-3}$ | $1.56^{E-3}$ | $1.44^{E-3}$ |
| $k_2$ ($s^{-1}$) | $2.88^{E-4}$ | $2.79^{E-4}$ | $2.58^{E-4}$ | $2.48^{E-4}$ | $2.51^{E-4}$ |
| $\Delta H_1$ (kJ $mol^{-1}$) | 1.66 | 1.56 | 1.51 | 1.35 | 1.01 |
| $\Delta H_2$ (kJ $mol^{-1}$) | 11.17 | 11.07 | 10.03 | 10.30 | 12.07 |
| $\Delta H_1 + \Delta H_2$ (kJ $mol^{-1}$) | 12.83 | 12.63 | 11.54 | 11.65 | 13.08 |
| $\Delta H_{Tmes}$ (kJ $mol^{-1}$) | 10.67 | 11.18 | 11.24 | 11.22 | 11.53 |

($\Delta H_1 + \Delta H_2$) enthalpy variations are close and even very close in some cases. The sum of the enthalpies deduced from the iteration at 90 °C (not reported) is also relatively close to that measured for this temperature.

## 5. Conclusion

Various techniques, as Raman, NMR or Mass Spectroscopies, were used to study the reaction of alkali solution on silica and let different interpretations. Microcalorimetry gave information on the heat effect of the process showing different steps occurring at different $Na_2O/SiO_2$ ratios. It also allowed proposing a kinetic scheme for low amounts of dissolved silica.

## Acknowledgment

The authors would like to thank the Tunisian Chemical Group (GCT) for financial support granted to Meriem Fertani-Gmati.

## References

[1] K. Jasmund, J. Geol. 66 (1952) 595–596.
[2] E.L. Brady, J. Phys. Chem. 57 (1953) 706–710.
[3] D. Bulteel, E. Garcia-Diaz, C. Vernet, H. Zanni, Cement Concrete Res. 32 (2002) 1199–1206.
[4] R.K. Iler, The Chemistry of Silica, Wiley, New York, 1979, 3–171.
[5] P.M. Dove, A. Crerar, Geochim. Cosmochim. Acta 54 (1990) 955–969.
[6] R. Dron, F. Brivot, Cement Concrete Res. 22 (1992) 941–948.
[7] N. Zotov, H. Keppler, Chem. Geol. 184 (2002) 71–82.
[8] C.E. Manning, Water–Rock Interaction I, 2004, pp. 45–52.
[9] J.A. Tossell, Geochim. Cosmochim. Acta 69 (2005) 283–291.
[10] G. Icopini, S. Brantley, P. Heaney, Geochim. Cosmochim. Acta 69 (2005) 293–303.
[11] N. Ingri, Acta Chem. Scand. 13 (1959) 758–775.
[12] G. Lagerstrom, Acta Chem. Scand. 13 (1959) 722–736.
[13] R.K. Harris, C.T.G. Knight, W.E. Hull, J. Am. Chem. Soc. 103 (1981) 1577–1578.
[14] S.A. Pelster, W. Schrader, F.J. Schuth, J. Am. Chem. Soc. 128 (2006) 4310–4317.
[15] J.P. Hershey, F.J. Millero, Marine Chem. 18 (1986) 101–105.
[16] M. Azaroual, C. Fouillac, J.M. Matray, Chem. Geol. 140 (1997) 155–165.
[17] S. Sjoberg, J. Noncrystal. Solids 196 (1996) 51–57.
[18] A.R. Felmy, H. Cho, J.R. Rustad, M.J. Mason, J. Sol. Chem. 30 (2001) 509–525.
[19] T.T. Trinh, A.P.J. Jansen, R.A. Van Santen, J. Phys. Chem. B 110 (2006) 23099–23106.

[20] K. Brahim, I. Khattech, J.P. Dubès, M. Jemal, Thermochim. Acta 436 (2005) 43–50.
[21] K. Antar, K. Brahim, M. Jemal, Thermochim. Acta 449 (2006) 35–41.
[22] K. Antar, M. Jemal, Thermochim. Acta 474 (2008) 32–35.
[23] M. Avrami, J. Chem. Phys. 7 (1939) 1103–1112.
[24] J. Kabai, Acta Chim. Acad. Sci. Hung. 78 (1973) 57–73.
[25] M.A. Wells, R.J. Gilkes, R.W. Fitzpatrick, Clays Clay Miner. 49 (2001) 60–72.
[26] M. Miyake, M. Maeda, Metall. Mater. Trans. B 37 B (2006) 181–188.
[27] M.S. Yavuz, H. Maedo, J. Alloys Compd. 28 (1998) 280–289.
[28] G.L. Perlovich, A. Bauer-Brandl, J. Therm. Anal. Calorim. 63 (2001) 653–661.
[29] M.S. Liu, Q. Zhao, Polymer 44 (2003) 2537–2545.
[30] A.K. Galwey, Thermochim. Acta 397 (2003) 249–268.
[31] S. Vyazovkin, Thermochim. Acta 397 (2003) 269–271.
[32] A. Khawam, D.R. Flanagan, Thermochim. Acta 429 (2005) 93–102.
[33] N.S. Sbirrazzuoli, D. Brunel, L. Elegant, J. Therm. Anal. 38 (1992) 1509–1524.
[34] S. Vyazovkin, J. Comput. Chem. 18 (1997) 393–402.
[35] S.V. Vyazovkin, Thermochim. Acta 236 (1994) 1–13.
[36] S.V. Vyazovkin, A.I. Lesnikovich, Thermochim. Acta 165 (1990) 273–280.